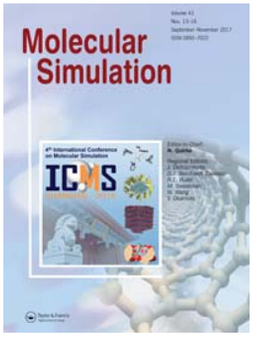

Molecular Simulation

ISSN: 0892-7022 (Print) 1029-0435 (Online) Journal homepage: http://www.tandfonline.com/loi/gmos20

A QM/MM study on the correlation between the polarisations of and electrons in a hydrated benzene

Daiki Suzuoka, Hideaki Takahashi & Akihiro Morita

To cite this article: Daiki Suzuoka, Hideaki Takahashi & Akihiro Morita (2017) A QM/MM study on the correlation between the polarisations of and electrons in a hydrated benzene, Molecular Simulation, 43:13-16, 1209-1217, DOI: 10.1080/08927022.2017.1350661

To link to this article: https://doi.org/10.1080/08927022.2017.1350661

MOLECULAR SIMULATION, 2017
VOL. 43, NOS. 13–16, 1209–1217
https://doi.org/10.1080/08927022.2017.1350661

Taylor & Francis
Taylor & Francis Group

A QM/MM study on the correlation between the polarisations of π and σ electrons in a hydrated benzene

Daiki Suzuoka[a], Hideaki Takahashi[a] and Akihiro Morita[a,b]

[a]Department of Chemistry, Graduate School of Science, Tohoku University, Sendai, Japan; [b]Elements Strategy Initiative for Catalysis and Batteries (ECISB), Kyoto University, Kyoto, Japan

ABSTRACT

In a recent work, we performed free-energy analyses for hydration of benzene by conducting QM/MM-ER simulations, where the total solvation free energy $\Delta\mu$ was decomposed into contributions $\Delta\overline{\mu}$ and $\delta\mu(\Delta\mu = \Delta\overline{\mu} + \delta\mu)$. $\Delta\overline{\mu}$ is the solvation free energy of the solute with a fixed electron density and $\delta\mu$ is the residual free energy due to the electron density polarisation in solution. We, further, decomposed the free energies $\delta\mu$ due to electron density fluctuations in aromatic solutes in aqueous solutions into contributions from π and σ orbitals. We note, however, that the decompositions will not be validated when the polarisations of π orbitals seriously couple with those of σ orbitals. In this paper, we study a correlation matrix between polarisations of π and σ orbitals through QM/MM simulations to assess the coupling strength among the orbitals. We found that the electron density polarisation is dominated by the polarisation arising from $\pi - \pi^*$ transfers between the orbitals lying in the HOMO–LUMO region. Thus, the polarisation of π electrons hardly couples with that from σ orbitals, which justifies our decomposition analyses.

ARTICLE HISTORY
Received 1 February 2017
Accepted 25 June 2017

KEYWORDS
QM/MM-ER; second-order perturbation theory; solvation free energy; XH/π interaction; correlation matrix

1. Introduction

In a solvation process, a solute molecule will be stabilised through its electron density polarisation in solution. In a polar solvent in particular, the polarisation effect gives a major contribution to the solvation free energy of the solute. It is well recognised that π electrons in aromatic compounds form intermolecular bondings referred to as 'XH/π interaction' with surrounding XH groups (X = C, N, or O) [1–6]. The major source of the XH/π interaction is considered as the van der Waals interaction or the dipole–dipole interaction between the polarised π electrons in the solute and the σ bonds in the environment. The XH/π interaction is known to play an essential role in a variety of phenomena in condensed phases, for instance, molecular stacking [7–9], molecular recognition, and protein folding [5,10–12]. However, the statistical properties of the XH/π interaction in condensed phases have not been well investigated so far on the quantitative basis.

Benzene has a slightly negative hydration free energy (−0.87 kcal/mol) [13,14], though it is a representative non-polar aromatic solute. The affinity of benzene to bulk water is, thus, considered as an implication of the OH/π interaction between benzene and water molecules. In our recent study [15], we carried out free-energy analyses for the hydration of benzene using QM/MM-ER method [16,17], which combines the quantum mechanical/ molecular mechanical (QM/MM) approach [18–20] with the theory of energy representation (ER) [21]. In QM/MM-ER the total solvation free energy $\Delta\mu$ is being decomposed into contributions $\Delta\overline{\mu}$ and $\delta\mu$, thus, $\Delta\mu = \Delta\overline{\mu} + \delta\mu$. $\Delta\overline{\mu}$ is the free energy associated with a transfer of a solute with fixed electron density $\widetilde{n}$ from gas phase to a solution of interest. $\delta\mu$ is the residual free energy due to electron density polarisation of the solute in solution. It was revealed that the free energy $\delta\mu$ is the major source of the affinity of benzene to bulk water. Further, in Ref. [15], we formally decomposed the free energy $\delta\mu$ into contributions $\delta\mu_\pi$ and $\delta\mu_\sigma$ due, respectively, to the fluctuation of π and σ electrons($\delta\mu = \delta\mu_\pi + \delta\mu_\sigma$). We found that the free energy $\delta\mu_\pi$ gives a dominant contribution to the hydration free energy of the solute. We note, however, that the validity of the free-energy decomposition should be examined carefully because the polarisation of the π electrons more or less couples with that of the σ orbitals. In this paper, we assess the strength of couplings among the orbitals by analysing a correlation matrix of polarisation energies of orbitals obtained through QM/MM simulations. To this end, the polarisation energy of each orbital in a QM solute is defined by means of the second-order perturbation approach (PT2) as done in Ref. [22].

The organisation of this paper is as follows. In the next section, we present the brief review of the QM/MM-ER method combined with the PT2 approach (QM/MM-PT2) and the method of the free-energy decompositions on the basis of a solution theory. We also introduce the correlation matrix for the polarisation energies of orbitals. Then, the computational details for the correlation analyses for π-electrons systems, i.e. ethene, benzene and phenylmethylether(PME) are provided in 'Computational Details'. In the section of 'Results and Discussion'

CONTACT Hideaki Takahashi hideaki@m.tohoku.ac.jp

we present the results of the QM/MM-PT2 simulations and discuss the validity of the free-energy decomposition analyses. We make a conclusion at the final section.

2. Theory and methodology

2.1. QM/MM-ER method combined with PT2 approach

Throughout this paper, we consider QM/MM systems where a solute molecule is described with a method of quantum chemistry and solvent molecules are represented with a classical force field. Within the QM/MM approach, the total energy $E_{\rm tot}$ of the whole system is written as

$$E_{\rm tot} = E_{\rm QM} + E^{\rm ES}_{\rm QM/MM} + E^{\rm vdW}_{\rm QM/MM} + E_{\rm MM}. \tag{1}$$

In Equation (1), $E_{\rm QM}$ is the electronic energy of the QM solute and $E_{\rm MM}$ is the energy of the MM solvent. $E^{\rm ES}_{\rm QM/MM}$ and $E^{\rm vdW}_{\rm QM/MM}$ are, respectively, the electrostatic and the van der Waals interaction between solute and solvent. In the following we assume that the coordinates of the solute are frozen during the simulation and we denote the instantaneous solvent coordinates collectively by $\mathbf{X}$.

We apply the second-order perturbation approach (PT2) to the QM/MM method in the same way as demonstrated in Ref. [15]. The perturbation $\mathbf{V}'_{\rm pc}[\mathbf{X}]$ is defined as the deviation of the electrostatic potential $\mathbf{V}_{\rm pc}[\mathbf{X}]$ formed by point charges on the solvent molecules from its average potential $\widetilde{\mathbf{V}}_{\rm pc}$ in solution, thus, $\mathbf{V}'_{\rm pc}[\mathbf{X}] = \mathbf{V}_{\rm pc}[\mathbf{X}] - \widetilde{\mathbf{V}}_{\rm pc}$. With the Rayleigh–Schrödinger perturbation theory, the energy $E_{\rm QM} + E^{\rm ES}_{\rm QM/MM}$ in Equation (1) can be expanded in a series,

$$E_{\rm QM} + E^{\rm ES}_{\rm QM/MM} = E^{(0)} + E^{(1)} + E^{(2)} + \cdots. \tag{2}$$

The energy $E^{(0)}$ in Equation (2) is the ground-state energy for the potential $\widetilde{\mathbf{V}}_{\rm pc}$ and independent of the solvent coordinates $\mathbf{X}$. $E^{(1)}$ is the electrostatic interaction between the ground-state density for $\widetilde{\mathbf{V}}_{\rm pc}$ and the solvent point charges. The sum of the second and higher order terms in Equation (2) describes the energy change due to polarisation of the solute in response to the solvent dynamics. We introduce the polarisation energy η defined by

$$\eta = E_{\rm tot}[n[\mathbf{X}], \mathbf{X}] - E_{\rm tot}[\widetilde{n}, \mathbf{X}] \tag{3}$$

where $n[\mathbf{X}]$ and $\widetilde{n}$ are the ground-state electron densities for the potential $\mathbf{V}_{\rm pc}[\mathbf{X}]$ and $\widetilde{\mathbf{V}}_{\rm pc}$, respectively. It is worthy of note that the polarisable continuum model approach (PCM) [23] can realise the reaction field $\widetilde{\mathbf{V}}_{\rm pc}$ at most and any asymmetric electric field formed by an instantaneous solvent configuration cannot be described with the method. If the perturbation expansion in Equation (2) is truncated at the second-order (PT2), η is identical to the second-order energy $E^{(2)}\left(\eta = E^{(2)}\right)$ [15,22]. With the unperturbed one-electron wave functions $\left\{\phi_i^{(0)}\right\}$ and their eigen energies $\left\{\epsilon_i^{(0)}\right\}$, $E^{(2)}$ is represented as

$$E^{(2)} = \sum_i^{\rm occ}\left(\sum_a^{\rm vir}\frac{\left|\left\langle\phi_i^{(0)}\middle|\,\mathbf{V}'_{\rm pc}\,\middle|\phi_a^{(0)}\right\rangle\right|^2}{\epsilon_i^{(0)} - \epsilon_a^{(0)}}\right) = \sum_i^{\rm occ}\eta_i. \tag{4}$$

In Equation (4), it is easy to see that η_i represents the polarisation energy of ith occupied orbital.

For the calculation of the solvation free energy $\Delta\mu$, we apply the QM/MM-ER method combined with the PT2 approach [15,22]. In the QM/MM-ER method [15–17,22], the solvation free energy $\Delta\mu$ is decomposed into the solvation free energy $\Delta\overline{\mu}$ of a solute with the fixed electron density $\widetilde{n}$ and the residual contribution $\delta\mu$ originating from the electron density fluctuation of the solute molecule in solution($\Delta\mu = \Delta\overline{\mu} + \delta\mu$). We refer to the system as the solution system when the electron density of the solute is determined under the influence of the interaction $\mathbf{V}_{\rm pc}[\mathbf{X}]$, while the system is referred to as the reference system when the electron density of the solute is fixed at the distribution $\widetilde{n}$. Since our major concern in the present work is placed on the electron density fluctuation of a solute in solution, the details of the method to compute $\Delta\overline{\mu}$ will not be described in this paper. Instead, we present below a brief review for the QM/MM-ER method. We refer the readers for details to the previous papers [16,21]. The free energy $\Delta\overline{\mu}$ is the solvation free energy of a solute with a fixed density $\widetilde{n}$ into MM solvent molecules, and expressed as

$$\exp\left(-\beta\Delta\overline{\mu}\right) = \frac{\int \mathrm{d}\mathbf{X}\ \exp\left[-\beta\left(E^{(0)} + E^{(1)}[\mathbf{X}] + E^{\rm vdW}_{\rm QM/MM}[\mathbf{X}] + E_{\rm MM}[\mathbf{X}]\right)\right]}{\int \mathrm{d}\mathbf{X}\ \exp\left[-\beta\left(E_0 + E_{\rm MM}[\mathbf{X}]\right)\right]} \tag{5}$$

where E_0 is the ground-state energy of the solute at isolation. The dependence of each term on the solvent coordinate $\mathbf{X}$ is explicitly shown in the equation. We note that E_0 as well as $E^{(0)}$ are constant and independent on the coordinate $\mathbf{X}$. The solute–solvent interaction $E^{(1)} + E^{\rm vdW}_{\rm QM/MM}$ in Equation (5) is pairwise since the electron density of the solute is frozen. Then, the free energy $\Delta\overline{\mu}$ can be computed straightforwardly employing a free-energy functional of the method of energy representation(ER) [21,24]. The ER method is based on the rigorous framework of the theory of solutions, where a distribution function of the solute–solvent interaction potential serves as a fundamental variable in density functional theory. Within the PT2 theory the free energy $\delta\mu$ due to the electron density polarisation around $\widetilde{n}$ is explicitly defined as

$$\exp\left(-\beta\delta\mu\right) = \frac{\int \mathrm{d}\mathbf{X}\ \exp\left[-\beta\left(E^{(0)} + E^{(1)} + E^{(2)} + E^{\rm vdW}_{\rm QM/MM} + E_{\rm MM}\right)\right]}{\int \mathrm{d}\mathbf{X}\ \exp\left[-\beta\left(E^{(0)} + E^{(1)} + E^{\rm vdW}_{\rm QM/MM} + E_{\rm MM}\right)\right]} \tag{6}$$

where β is the inverse of Boltzmann constant $k_{\rm B}$ multiplied by temperature T. It is easy to see that the sum of the free energies $\Delta\overline{\mu}$ and $\delta\mu$ defined, respectively, in Equations (5) and (6) constitutes the free energy $\Delta\mu$. It should be noted that the

free energy $\delta\mu$ is, of course, dependent on the choice of the reference state. In the present work we take $\widetilde{n}$ as the reference since we are interested in the electron density polarisation from the density $\widetilde{n}$ corresponding to the average potential $\widetilde{\mathbf{V}}_{\mathrm{pc}}$. For the computation of the free energy $\delta\mu$ within the framework of the energy representation, we introduce the energy distribution functions for the energy coordinate η defined in Equation (3). In terms of the distribution functions $\rho(\eta)$ and $\rho_0(\eta)$ constructed, respectively, in the solution and the reference systems, the functional for the free energy $\delta\mu$ is given by [17]

$$\delta\mu = \int \mathrm{d}\eta \left(k_{\mathrm{B}}T \ln\left(\frac{\rho(\eta)}{\rho_0(\eta)}\right) + \eta \right) W(\eta) \tag{7}$$

where W is a normalised weight function. Choice of W only slightly affect the value of $\delta\mu$ and can be constructed to reduce the statistical error in evaluating $\delta\mu$. We adopt an equation proposed in Ref. [25]. As shown in Equation (4) the energy $E^{(2)}$ is given by sum of the contributions from occupied orbitals. Hence, it is quite straightforward to decompose the polarisation energy $\eta = E^{(2)}$ to the contributions from π and σ orbitals, thus,

$$E^{(2)} = \eta_\pi + \eta_\sigma = \sum_{i\in\pi}^{\mathrm{occ}} \eta_i + \sum_{j\in\sigma}^{\mathrm{occ}} \eta_j. \tag{8}$$

With the distribution functions $\rho_\pi(\eta_\pi)$ and $\rho_{0,\pi}(\eta_\pi)$ in solution and reference systems, respectively, $\delta\mu_\pi$ is expressed as

$$\begin{aligned}\delta\mu_\pi = \int \mathrm{d}\eta_\pi \Big[&\left(\rho_\pi(\eta_\pi) - \rho_{0,\pi}(\eta_\pi)\right) + \beta\omega_\pi(\eta_\pi)\rho_\pi(\eta_\pi) \\ &- \beta\int_0^1 \mathrm{d}\lambda\omega_\pi(\eta_\pi;\lambda)\left(\rho_\pi(\eta_\pi) - \rho_{0,\pi}(\eta_\pi)\right)\Big]\end{aligned} \tag{9}$$

with a similar expression for $\delta\mu_\sigma$. In Equation (9) λ denotes the coupling parameter describing the polarisation of the solute and varies from $\lambda = 0$ (reference system) to $\lambda = 1$ (solution system). ω_π in Equation (9) represents the indirect part of the solute–solvent interaction of mean force and is given by

$$\omega_\pi(\eta_\pi) = -k_{\mathrm{B}}T \ln\left(\frac{\rho_\pi(\eta_\pi)}{\rho_{0,\pi}(\eta_\pi)}\right) - \eta_\pi. \tag{10}$$

It is important to note that the potential ω_π carries the effect of the complicated correlation among π and σ electrons in the solute of interest. Equation (9) can be derived from the Kirkwood charging formula [26] with the definition of the potential ω of Equation (10) represented on the energy coordinate. In Equation (9), integration of ω_π with respect to λ is carried out using PY approximation combined with HNC formula [26]. In the PY and HNC approximations, it is assumed that the exponential of potential ω and potential ω itself are dependent linearly on the coupling parameter λ, respectively. We, thus, realise the free-energy decomposition of $\delta\mu = \delta\mu_\pi + \delta\mu_\sigma$. In the following, we discuss the validity of this decomposition by analysing the correlation among the polarisations of the π and σ electrons.

2.2. Analysis of orbital correlation

Here, we introduce a matrix χ to analyse correlation between the polarisations of orbitals in solution. The correlation matrix $\chi_{\pi\sigma}$ between π and σ orbitals is defined using the polarisation energies η_π and η_σ in Equation (8) as

$$\chi_{\pi\sigma}(\eta_\pi, \eta_\sigma) = -k_{\mathrm{B}}T \frac{\delta\rho_\pi(\eta_\pi)}{\delta V_\sigma(\eta_\sigma)}. \tag{11}$$

In Equation (11), $\chi_{\pi\sigma}$ represents the linear response of the distribution ρ_π with respect to the potential shift δV_σ due to polarisation of the σ electrons. We note that $V_\sigma(\eta_\sigma) = \eta_\sigma$ holds in Equation (11). The function $\chi_{\pi\sigma}(\eta_\pi, \eta_\sigma)$ can be considered as a matrix of which arguments η_π and η_σ are continuous.

To describe the potential ω_π in Equation (10) in terms of contributions due to the self-correlation term and the cross term, we derive an alternative representation of Equation (11) as

$$\delta\rho_\pi(\eta_\pi) = -\beta \int \mathrm{d}\eta_\sigma \chi_{\pi\sigma}(\eta_\pi, \eta_\sigma)\eta_\sigma. \tag{12}$$

Equation (12) states that the distribution shift $\delta\rho_\pi(\eta_\pi)$ associated with the potential shift $\delta V_\sigma(\eta_\sigma) = \eta_\sigma$ can be evaluated by the correlation matrix $\chi_{\pi\sigma}$ within the linear response regime. Then, it is possible to decompose the shift $\delta\rho_\pi$ into contributions from self terms and from cross terms between π and σ orbitals, thus,

$$\begin{aligned}\delta\rho_\pi(\eta_\pi) &= \delta\rho_{\pi\pi}(\eta_\pi) + \delta\rho_{\pi\sigma}(\eta_\pi) \\ &= -\beta\Big(\int \mathrm{d}\eta'_\pi \chi_{\pi\pi}(\eta_\pi, \eta'_\pi)\eta'_\pi \\ &\quad + \int \mathrm{d}\eta'_\sigma \chi_{\pi\sigma}(\eta_\pi, \eta'_\sigma)\eta'_\sigma \Big)\end{aligned} \tag{13}$$

where the notation η' is just introduced to represent the off-diagonal elements of the matrix. The first term $\delta\rho_{\pi\pi}$ in Equation (13) is obviously the contribution due to the self-correlation within π electrons and the second term $\delta\rho_{\pi\sigma}$ describes the density shift resulting from the orbital correlation $\chi_{\pi\sigma}$ between π and σ electrons. Similarly, $\delta\rho_\sigma$ can also be decomposed into the self term $\delta\rho_{\sigma\sigma}$ and the cross term $\delta\rho_{\sigma\pi}$. By substituting the expression of Equation (13) to Equation (10) we have

$$\begin{aligned}\omega_\pi(\eta_\pi) \approx \frac{1}{\rho_{0,\pi}(\eta_\pi)} \Big[&\int \mathrm{d}\eta'_\pi \chi_{\pi\pi}(\eta_\pi, \eta'_\pi)\eta'_\pi \\ &+ \int \mathrm{d}\eta'_\sigma \chi_{\pi\sigma}(\eta_\pi, \eta'_\sigma)\eta'_\sigma \Big] - \eta_\pi.\end{aligned} \tag{14}$$

In deriving Equation (14), we expand a logarithm part of ω_π in Equation (10) into power series of $\delta\rho_\pi$ and truncate it at the first order. From Equation (14) we find that ω_π includes the contribution from σ electrons represented by the correlation matrix $\chi_{\pi\sigma}$. When the contribution of the off-diagonal block $\chi_{\pi\sigma}$ is much smaller than that of the self-correlation $\chi_{\pi\pi}$, it is reasonable to regard that $\delta\mu_\pi$ in Equation (9) is dominated by π electrons.

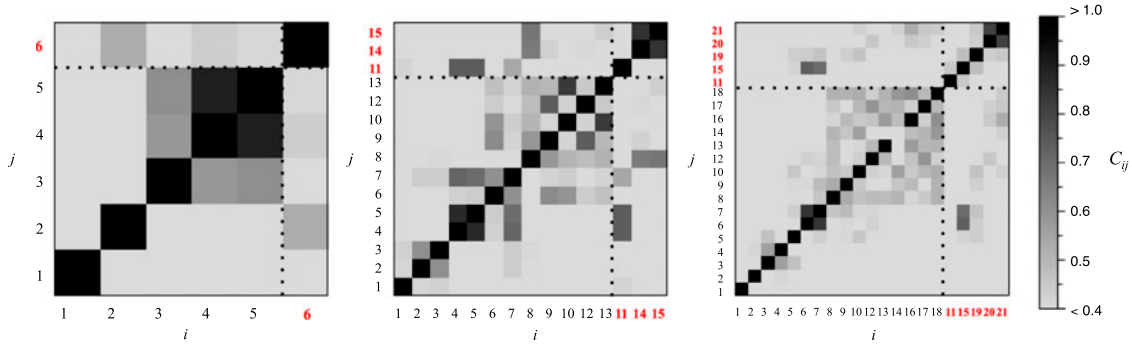

Figure 1. (Colour online) Orbital correlation matrices C_{ij} for (a) ethene, (b) benzene and (c) phenylmethylether in water solutions. The indices i and j represent the serial numbers of valence orbitals in ascending order of eigenvalues. Bold and red numbers denote π orbitals and dotted lines show the boundaries between the groups of π and σ orbitals.

It is also straightforward to define the specific correlation $\chi_{ij}(\eta_i, \eta_j)$ for the orbital polarisation energies η_i and η_j defined in Equation (4). $\chi_{ij}(\eta_i, \eta_j)$ can be constructed through a QM/MM simulation using the formula,

$$\chi_{ij}(\eta_i, \eta_j) = \left\langle \hat{\rho}_i(\eta_i)\, \hat{\rho}_j(\eta_j) \right\rangle_0 - \rho_{0,i}(\eta_i)\, \rho_{0,j}(\eta_j). \tag{15}$$

In Equation (15), $\hat{\rho}_i$ is the instantaneous distribution function of the polarisation energy η_i and $\langle \cdots \rangle_0$ represents the ensemble average taken in the reference system. To evaluate the correlation strength for the orbital pair (i, j) we introduce in this paper the quantity C_{ij} defined as

$$C_{ij} = \int \mathrm{d}\eta_i \mathrm{d}\eta_j \left| \chi_{ij}(\eta_i, \eta_j) \right|. \tag{16}$$

Similarly, we can also construct the correlation matrix $\chi_{\pi\sigma}(\eta_\pi, \eta_\sigma)$ and $C_{\pi\sigma}$ for the polarisation energies η_π and η_σ defined in Equation (8). As shown in Appendix 1 it is possible to prove that C_{ij} in Equation (16) ranges from 0.0 to 2.0.

3. Computational details

In this paper, we study the free energy $\delta\mu$ in the hydration of benzene, ethene and phenylmethylether (PME) by performing the QM/MM-ER simulations combined with the PT2 approach (QM/MM-PT2). The details for the method are provided in Ref. [15].

The geometry optimisations for the solute molecules are performed with the polarisable continuum model (PCM) [23] in Gaussian 09 package [27] at the B3LYP/aug-cc-pVTZ level [28, 29]. The solute molecules are fixed at their optimised geometries during the QM/MM-PT2 simulations.

To construct the zeroth-order wave functions $\left\{\phi_i^{(0)}\right\}$ and eigenvalues $\left\{\epsilon_i^{(0)}\right\}$ for the average electrostatic potential $\widetilde{\mathbf{V}}_{\mathrm{pc}}$, we employ the Kohn–Sham density functional theory (DFT) [30,31] using the real-space-grid technique [32–36]. The wave functions are confined within a cubic QM cell where the number of the grid points along each axis is set at 64 with the grid spacing $h = 0.152$ Å. The kinetic energy operators are approximated by fourth-order finite-difference method proposed by Chelikowsky, et al. [32,33] and the interactions between valence electrons and nuclei are evaluated by pseudopotentials in the form developed by Kleinman and Bylander [37]. Near the atomic core regions, we introduce the double grids [38], where the width of the dense grid is set at 0.2 h. The exchange-correlation energies are calculated by the BLYP functional [39,40] since the use of B3LYP functional in the QM/MM simulation is rather time consuming. Fortunately, the solute–solvent interaction is only weakly dependent on the choice of the functional as long as the solute is neutral and less polarisable. In the summation of Equation (4), we consider the virtual orbitals whose eigenvalues are less than 0.2 a.u. The MM subsystem consists of about 500 water molecules contained within a cubic simulation box($L = 24.6$ Å) with periodic boundary conditions [41,42]. The constant-NVT molecular dynamics simulations are performed by rescaling velocities [41,42]. The water molecules are described by SPC/E model [43]. The equations of motions are solved numerically by the leap–frog algorithm [41,42] with the time step of 1.0 fs. The internal coordinates of the water molecules are fixed during the simulations and the rotational motions are described using quaternion. [41,42] The Ewald method [41,42] is used for the calculation of the solvent–solvent Coulomb interactions. To evaluate the van der Waals interaction between the QM and MM subsystems, we adopt the GROMOS43A1 model [44] for benzene and OPLS-AA [45] for other solute molecules. The specific use of GROMOS43A1 parameter for benzene is intended to realise a negative solvation free energy since it employs the relatively small size parameters. The thermodynamic condition of the solution is set at temperature $T = 300$ K and water density $\rho = 1.0$ g/cm^3.

The averaged electrostatic field $\widetilde{\mathbf{V}}_{\mathrm{pc}}$ for each solute is obtained by performing the conventional QM/MM simulation for 500 ps in a solution system. Then, the reference density $\widetilde{n}$ is given as the ground-state density of the Kohn–Sham equation that involves $\widetilde{\mathbf{V}}_{\mathrm{pc}}$ as a reaction field. The computational set-up for solving the Kohn–Sham equation with the real-space-grid technique is the same as described above. The solvation free energies $\Delta\overline{\mu}$ for the solutes with the frozen electron density $\widetilde{n}$ were those

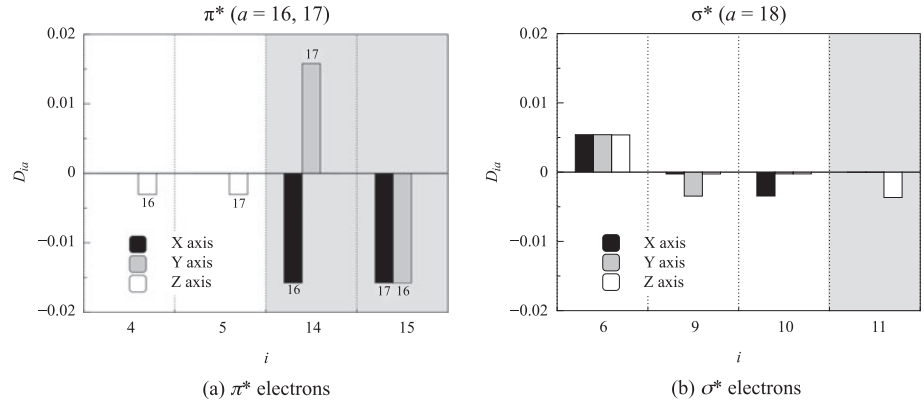

Figure 2. Orbital coupling strength D_{ia} (Equation (19)) between ith occupied orbital and ath virtual orbital in benzene for the applied electric fields parallel to x, y and z axes. x axis is aligned parallel to a CH bond in benzene. (a) D_{ia} for the transfers to π^* orbitals ($a = 16, 17$), (b) D_{ia} for the transfers to σ^* orbitals ($a = 18$). The regions with white and grey backgrounds correspond to σ and π occupied orbitals, respectively. The D_{ia} values of which absolutes are larger than 10^{-3} are shown.

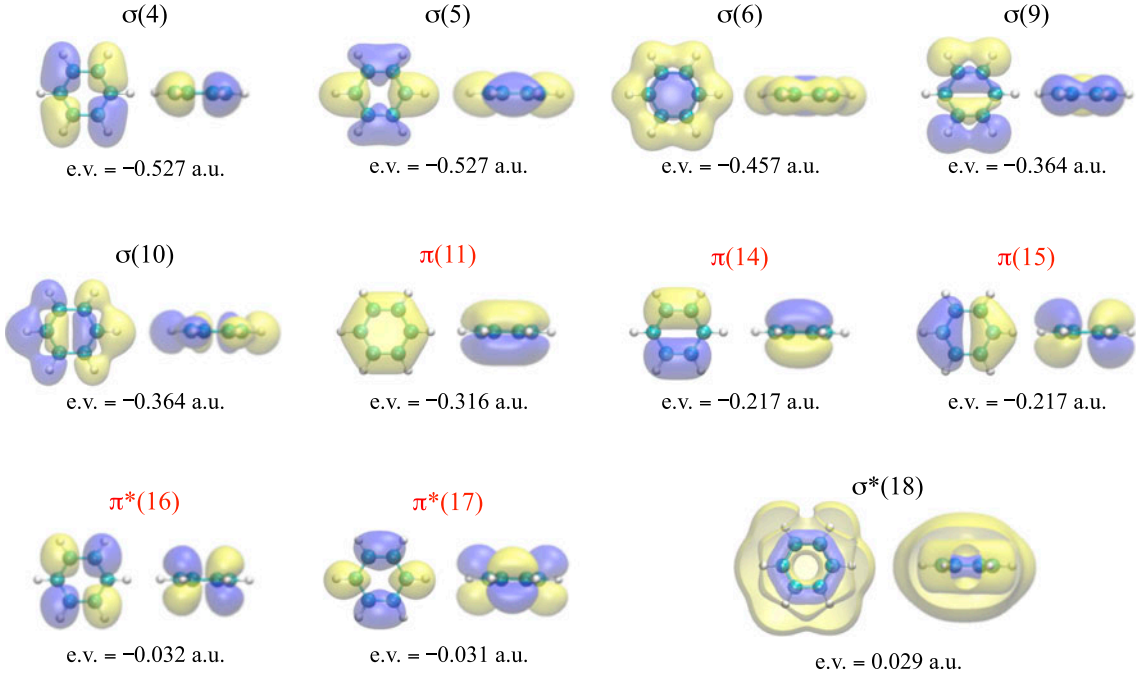

Figure 3. (Colour online) Three-dimensional contour surfaces for the Kohn–Sham orbitals φ_i in benzene placed in an average potential $\tilde{\mathrm{V}}_{\mathrm{pc}}$. The orbitals appearing in Figure 2 are depicted. In each figure the left is a top view and the right is a side view. The eigen value (e.v.) is also shown at the bottom of each orbital. The values of the contour surfaces are ±0.02 a.u. Contour surface of $\sigma^*(18)$ orbital is cut off at the front of the surface.

evaluated in Ref. [15]. The statistics to construct the energy distribution functions for $\Delta\overline{\mu}$ was precisely described in Section 3.4 of Ref. [15]. The free-energy functional for $\Delta\overline{\mu}$ was given in Equation (12) in Ref. [16]. Thus, $\Delta\overline{\mu}$ including long-range correction were computed as +2.32, +0.84, and −0.13 kcal/mol for ethene, benzene, and phenylmethylether(PME), respectively [15]. The QM/MM-PT2 simulations are carried out for 200 ps to construct the distributions $\rho(\eta)$ and $\rho_0(\eta)$ in the solution and reference systems, respectively. These distribution functions are served as variables to the free-energy functionals given in Equations (7) and (9). For the construction of the correlation matrix $\chi_{ij}(\eta_i, \eta_j)$ in Equation (15), we also perform 200-ps QM/MM-PT2 simulations.

4. Results and discussion

4.1. Correlation matrix

Figure 1 shows the two-dimensional representations of the orbital correlation matrices $\{C_{ij}\}$ for (a) ethene, (b) benzene and (c) phenylmethylether (PME), where the valence orbitals are arranged in groups of σ and π orbitals in ascending order of their orbital energies. The vertical and horizontal dotted lines show the boundaries between σ and π orbital groups. Then, the upper right area corresponds to the $\pi - \pi$ couplings, while the lower left represents the correlations among σ orbitals. The remaining rectangular blocks are responsible for the cross couplings between σ and π orbitals. The diagonal elements

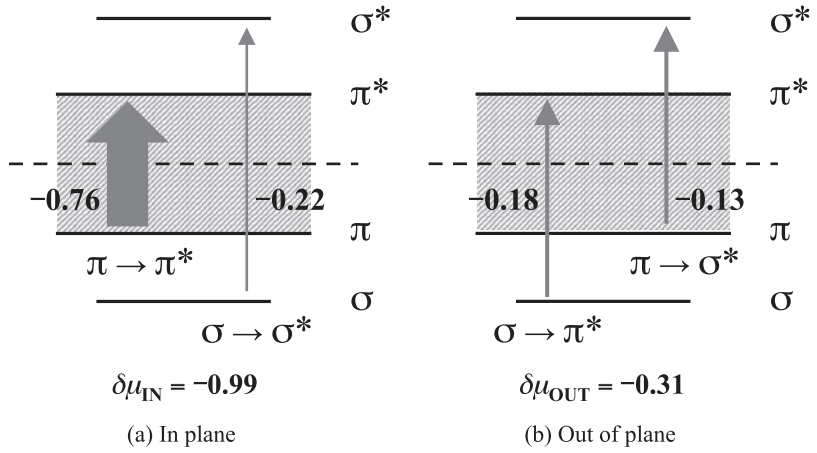

Figure 4. Schematic illustration of the energy levels of the orbitals in benzene. The arrows represent the electronic transfers which cause the density polarisations given by Equation (17) in response to uniform electric fields applied (a) parallel and (b) perpendicular to the molecular plane of benzene. The area neighbouring HOMO and LUMO (meshed area) contains mostly π and π^* orbitals. The values attached to the arrows are the corresponding free energies in units of kcal/mol. Width of an arrow schematically shows the degree of the orbital coupling for the transfer.

correspond to self-correlations of orbitals, and all of these values were estimated as almost 2.0 (see Appendix 1). At first glance on the figures, it is recognised in the correlation matrices for the three π electrons systems that the block diagonal portions are dominant suggesting relatively weak $\pi - \sigma$ couplings.

First, we discuss the correlation in benzene molecules as a representative of π electron system. In Figure 1(b) we observe that some non-negligible values are present in $\sigma - \pi$ pairs, for instance, $\sigma(4) - \pi(11)$ and $\sigma(5) - \pi(11)$, for which the correlations were evaluated as $C_{4\text{-}11} = 0.74$ and $C_{5\text{-}11} = 0.74$, respectively. To quantify the strength of the overall $\sigma - \pi$ coupling, we construct the 2×2 correlation matrix using Equation (16) for the energy coordinates η_π and η_σ defined in Equation (8). We, then, found that the σ-π correlation $C_{\sigma\pi}$ was computed as 0.54 for benzene showing that the cross correlations are rather small as compared to the values of the self correlations $C_{\pi\pi}$ and $C_{\sigma\sigma}$ (≈ 2.0). These results suggest that the polarisations of the π electrons couple with those of σ electrons in hydration with relatively weak coupling strength as compared to self correlations. We see the similar situations in the polarisations of ethene and phenylmethylether(PME) as well. Actually, C_{2-6} for ethene, and C_{6-15} and C_{7-15} for PME have relatively larger values in the $\sigma - \pi$ coupling domains. We, thus, conclude that the free energy change $\delta\mu$ due to electron density fluctuation of the solute molecule expressed in Equation (7) can be reasonably decomposed into contributions from σ and π electrons. In the following subsection, we study the underlying mechanism responsible for the decoupling between σ and π electrons by applying uniform electric fields to a benzene molecule. We also make a remark on the dependence of the present results on the exchange-correlation functional in the DFT calculations. It is well known that a generalised gradient approximation(GGA) functional, e.g. BLYP used in the present QM/MM simulations significantly overestimates the polarisation of a long π−conjugated system induced by an electric field exerted along the longitudinal axis [46]. The addition of the exact Hartree–Fock (HF) exchange to the functional effectively suppresses the polarisation. Thus, a hybrid functional which partly involves the HF exchange overcomes a typical deficiency inherent in a GGA functional. In the present case, however, the size of the solute is rather small, and hence the effect of the functional on the polarisability is considered to be marginal.

4.2. Orbital polarisation by uniform electric field

To analyse the coupling between the orbital polarisations, we consider in this subsection the polarisation parallel and perpendicular to the molecular plane of benzene by applying uniform electric fields **F**. Within the PT2 theory, the polarisation density $n_{ia}^{(2)}$ due to $i \to a$ electronic transition via the electric field **F** is given by

$$n_{ia}^{(2)}(\mathbf{r}) = \frac{\left\langle \phi_i^{(0)} \left| \mathbf{U} - \widetilde{\mathbf{V}}_{\mathrm{pc}} \right| \phi_a^{(0)} \right\rangle}{\epsilon_i^{(0)} - \epsilon_a^{(0)}} \phi_i^{(0)}(\mathbf{r}) \phi_a^{(0)}(\mathbf{r}) \tag{17}$$

where **U** is the potential due to the field **F**. Hereafter, we use the term '$i \to a$ transfer' to describe the electronic polarisation due to the mixing of an electronic configuration in which an electron in an occupied orbital i in the ground-state configuration is transferred to a virtual orbital a. Then, the polarisation energy $E^{(2)}$ can be rewritten as the interaction of the polarisation density $n_{ia}^{(2)}$ with the perturbation, thus,

$$E^{(2)} = \sum_i^{\mathrm{occ}} \sum_a^{\mathrm{vir}} \int d\mathbf{r}\, n_{ia}^{(2)}(\mathbf{r}) \left(U(\mathbf{r}) - \widetilde{V}_{\mathrm{pc}}(\mathbf{r}) \right). \tag{18}$$

Here, we introduce the orbital coupling strength D_{ia} between ith occupied orbital and ath virtual orbital, thus,

$$D_{ia} = \frac{\left\langle \phi_i^{(0)} \left| \mathbf{U} - \widetilde{\mathbf{V}}_{\mathrm{pc}} \right| \phi_a^{(0)} \right\rangle}{\epsilon_i^{(0)} - \epsilon_a^{(0)}}. \tag{19}$$

Table 1. The free energies $\delta\mu$ due to electron density polarisations upon hydration are presented in units of kcal/mol for ethene, benzene and phenylmethylether(PME). Each $\delta\mu$ is decomposed into contributions due to in-plane($\delta\mu_{\rm IN}$) and out-of-plane($\delta\mu_{\rm OUT}$) polarisations. $\delta\mu_{\rm IN}$ is further decomposed into the free energies $\delta\mu_{\pi-\pi^*}$ and $\delta\mu_{\sigma-\sigma^*}$ caused by $\pi-\pi^*$ and $\sigma-\sigma^*$ transfers, respectively. Similarly $\delta\mu_{\rm OUT}$ is also given by sum of the free energies $\delta\mu_{\pi-\sigma^*}$ and $\delta\mu_{\sigma-\pi^*}$.

		$\delta\mu_{\rm IN}$			$\delta\mu_{\rm OUT}$		
Solute	$\delta\mu$	$\delta\mu_{\pi\text{-}\pi^*}$		$\delta\mu_{\sigma\text{-}\sigma^*}$	$\delta\mu_{\pi\text{-}\sigma^*}$		$\delta\mu_{\sigma\text{-}\pi^*}$
Ethene	−0.43		−0.30			−0.13	
		−0.14		−0.15	−0.06		−0.04
Benzene[a]	−1.30		−0.99			−0.31	
		−0.76		−0.22	−0.18		−0.13
PME[a]	−1.71		−1.17			−0.35	
		−0.87		−0.35	−0.21		−0.12

[a]Ref. [15].

It is readily understood that the quantity D_{ia} describes the magnitude of the polarisation due to $i \rightarrow a$ transfer in response to the potential $\mathbf{U}$.

We first consider the polarisation parallel to the molecular plane, that is, the density fluctuation induced by the electric field along the x or y axis. Figure 2 shows the values of D_{ia} for some orbital pairs (i, a). As shown in Equation (17) D_{ia} is an expansion coefficient for perturbation theory and is dimensionless. The l component ($l = x, y, z$) of D_{ia} can be directly evaluated by applying the electric field along the l direction. We note that orbital pairs having D_{ia} values less than 10^{-3} are omitted for the sake of simplicity. It is readily recognised in Figure 2(a) that π orbitals $\pi(14)$ and $\pi(15)$ favourably couple with $\pi^*(16)$ and $\pi^*(17)$ ($\pi-\pi^*$ transfer), resulting in substantial polarisations along the molecular plane. Thus, the π orbitals near HOMO are significantly polarised with strong mutual correlations because of rather small energy gaps related to the transfers. The transfer from $\sigma(6)$ to $\sigma^*(18)$ (Figure 2(b)) also makes some contribution to the polarisation. However, $\sigma(6)$ couples with $\sigma^*(18)$ equivalently for the electric fields applied to x, y, and z directions. Hence, its polarisation will not correlate with other orbitals. For references we present in Figure 3 the contour plots for the molecular orbitals related to the polarisations discussed here.

We next discuss the polarisation perpendicular to the molecular plane which arises from $\sigma-\pi^*$ or $\pi-\sigma^*$ transfers. We see in Figure 2(a) that $\sigma(4)$ and $\sigma(5)$ weakly couple with $\pi^*(16)$ and $\pi^*(17)$, respectively, by means of the electric field along the z direction. These polarisations correlate with the transfer from $\pi(11)$ to $\sigma^*(18)$ as shown in Figure 2(b) though the coupling is rather weak due to the intermediately large energy gap between the orbitals.

To summarise the polarisation discussed above, the related transfers are schematically illustrated in Figure 4(a) and (b). The polarisation along the molecular plane (Figure 4(a)) is governed by those arising from the $\pi-\pi^*$ transfers between the orbitals lying in the HOMO–LUMO region, which can hardly correlates with the polarisation due to $\sigma-\sigma^*$ transfers with larger energy gaps. On the other hand, when the electric field is applied to the z direction the polarisations due to $\pi-\sigma^*$ weakly couple with those arising from $\sigma-\pi^*$ transfers as shown in Figure 4(b). The coupling strength between these polarisations may be limited since the orbitals for the $\pi-\sigma^*$ or $\sigma-\pi^*$ transfers are intermediately separated in the energy level. Thus, the density polarisation arising from the π orbitals couples with that due to the σ orbitals mainly through the electric field along the z direction. Since the energy levels of the π and σ orbitals in ethene and PME are similar to those illustrated in Figure 4(a) and (b) the above discussion would also apply to these molecules.

4.3. Free-energy decomposition

The above discussion can be substantiated by the free-energy decompositions provided in our previous paper. [15] The free energy $\delta\mu_{\rm IN}$ arising from the in-plane polarisation was evaluated as −0.99 kcal/mol, in which the free energy $\delta\mu_{\pi-\pi^*}$ due to the $\pi-\pi^*$ transfers was found to give the major contribution (−0.76 kcal/mol) and the remaining contribution $\delta\mu_{\sigma-\sigma^*}$ was computed as −0.22 kcal/mol. These results are nicely consistent with the diagram shown in Figure 4(a) where the free-energy values are attached to the corresponding transfers. On the other hand, the free energy $\delta\mu_{\rm OUT}$ due to the out-of-plane polarisation (see Figure 4(b)) was computed as −0.31 kcal/mol, where the free energy $\delta\mu_{\sigma-\pi^*}$(− 0.18 kcal/mol) by the $\sigma-\pi^*$ transfers give contribution comparable to the free energy $\delta\mu_{\pi-\sigma^*}$(− 0.13 kcal/mol) by the $\pi-\sigma^*$ transfers. Similarly for PME as presented in Ref. [15] $\delta\mu_{\rm IN}$ was evaluated as −1.17 kcal/mol that is distinctly larger than the free energy $\delta\mu_{\rm OUT}$ = −0.35 kcal/mol. The same trend also applies to ethene, where $\delta\mu_{\rm IN}$ and $\delta\mu_{\rm OUT}$ were computed as −0.30 and −0.13 kcal/mol, respectively. These results are summarised in Table 1. It was, thus, quantified that the in-plane polarisation dominates the stabilisation due to the many-body interactions. We note that whole of the free energy $\delta\mu$ can be expressed by sum of the free energies $\delta\mu_{\rm IN}$ and $\delta\mu_{\rm OUT}$, thus, $\delta\mu = \delta\mu_{\rm IN} + \delta\mu_{\rm OUT} = -1.3$ kcal/mol. $\delta\mu$ can also be computed directly as −1.30 kcal/mol in terms of the distribution functions for the whole energy $\eta = E^{(2)}$ utilising the free-energy functional of Equation (7). The coincidence of these two values implies the robustness and the reliability of the free-energy decomposition. Similarly, we also found that sum of the free energies $\delta\mu_\pi = -0.94$ kcal/mol and $\delta\mu_\sigma = -0.35$ kcal/mol reasonably agrees with the free energy $\delta\mu$. In Ref. [47] the free-energy contribution due to electron density polarisation in benzene in water solution was evaluated as −0.9 kcal/mol. Since the reference density was taken as the electron density of the solute at isolation it cannot be directly compared with our result (−1.3 kcal/mol). However, the total solvation free energy $\Delta\mu = -0.56$ or −0.59 kcal/mol in Ref. [47] reasonably agrees with our result ($\Delta\mu = -0.47$ kcal/mol). In the present calculation as well as in Ref. [47] the solutes geometries were fixed during the QM/MM simulations.

Considering the vibration of the molecular geometry will slightly stabilise the free energy $\delta\mu$ and as a consequence the total solvation free energy of benzene will get closer to the experimental value(−0.87 kcal/mol).

5. Conclusion

The π electrons in an aromatic compound will play a role in hydration by forming 'OH/π interaction' with surrounding water molecules. In our recent work [15], we performed a set of QM/MM-ER simulations combined with second-order perturbation theory (PT2) to study quantitatively the role of the fluctuation of π and σ electrons in the hydration of benzene. By means of the free-energy decomposition analyses, it was revealed that the free energy $\delta\mu_\pi$ due to the polarisation of π electrons dominates the stabilisation of benzene in solution ($\delta\mu_\pi = -0.94$ kcal/mol). The major purpose of this paper is to examine the validity of the decomposition analyses by studying the matrix which represents the correlation among the polarisation of electrons on the π and σ orbitals.

We performed QM/MM simulations coupled with PT2 method to construct the correlation matrices for the polarisations of orbitals in the hydrated π-electrons systems, i.e. ethene, benzene, and phenylmethylether(PME). In these solutes, it was shown that the block-diagonal portion is dominant in the correlation matrices upon hydrations, implying relatively weak couplings between π and σ orbitals. In the hydration of benzene, it was revealed that the electron density fluctuation parallel to the molecular plane is dominated by the polarisations due to the $\pi - \pi^*$ transfers between the orbitals lying in the HOMO–LUMO region. The similar situation also applies to ethene and PME and as a consequence the free energy due to the electron density polarisation along the molecular plane surpasses the free energy due to polarisation perpendicular to molecular plane in these molecules. Thus, the polarisation of the σ electrons along the molecular plane can hardly couple with that of the π electrons due to relatively large energy gaps. Actually, the smallest $\pi - \pi^*$ gap for the reference state is evaluated as 0.186 a.u. for $\pi(14, 15)$ and $\pi^*(16)$, while the smallest $\sigma - \sigma^*$ gap is 0.322 a.u. for $\pi(12, 13)$ and $\sigma^*(18)$. For the application of the electric field perpendicular to the molecular plane, we found that the polarisation due to the $\pi - \sigma^*$ transfer weakly couples with that arising from the $\sigma - \pi^*$ transfers. However, the coupling strength is not significant since the orbitals related to the out-of-plane polarisation are intermediately separated in the energy level.

We conclude that the weak coupling between the polarisations of π and σ electrons in aqueous solution mainly arises from the solvent electric field perpendicular to the molecular plane of the benzene. We also note that these discussions are consistent with the quantitative results given in Ref. [15]. Our free-energy decomposition analyses was, thus, validated on the basis of the correlation matrix between the polarisations of π and σ electrons.

Disclosure statement

No potential conflict of interest was reported by the authors.

Funding

This work is supported by the Ministry of Education, Culture, Sports, Science, and Technology (MEXT) under the Grant-in-Aid for Scientific Research on Innovative Areas [grant number 23118701]; the Japan Society for the Promotion of Science (JSPS) under the Grant-in-Aid for Challenging Exploratory Research [grant number 25620004]; the Nanoscience Program and the Computational Materials Science Initiative of the Next-Generation Supercomputing Project (No. hp160007, hp160013, hp160019 and hp160214); JSPS Research Fellowships for Young Scientists [grant number JP16J02027].

ORCID

Hideaki Takahashi http://orcid.org/0000-0002-4412-4115

References

[1] Tamres M, Searles S, Leighly EM, et al. Hydrogen bond formation with pyridines and aliphatic amines. J Am Chem Soc. 1954;76:3983–3985.
[2] Nishio M, Hirota M, Umezawa Y. The CH/π interaction. New York (NY): Willey-VCH; 1998.
[3] Tsuzuki S, Honda K, Uchimaru T, et al. Origin of attraction and directionality of the π/π interaction: model chemistry calculations of benzene dimer interaction. J Am Chem Soc. 2002;124:104–112.
[4] Desiraju GR, Steiner T. The weak hydrogen bond. New York (NY): Oxford University Press; 1999.
[5] Chakrabarti P, Bhattacharyya R. Geometry of nonbonded interactions involving planar groups in proteins. Prog Biophys Mol Biol. 2007;95:83–137.
[6] Levitt M, Perutz MF. Aromatic rings act as hydrogen bond acceptors. J Mol Biol. 1988;201:751–754.
[7] Meyer EA, Castellano RK, Diederich F. Interactions with aromatic rings in chemical and biological recognition. Angew Chem Int Ed. 2003;42:1210–1250.
[8] Sun H, Tottempudi UK, Mottishaw JD, et al. Strengthening π-π interactions while suppressing C_{sp2}-H$\cdots\pi$ (T-shaped) interactions via perfluoroalkylation: a crystallographic and computational study that supports the beneficial formation of 1-D π-π stacked aromatic materials. Cryst Growth Des. 2012;12:5655–5662.
[9] Fujii A, Shibasaki K, Kazama T, et al. Experimental and theoretical determination of the accurate interaction energies in benzene-halomethane: the unique nature of the activated CH/π interaction of haloalkynes. Phys Chem Chem Phys. 2008;10:2836–2843.
[10] Steiner T, Schreurs AMM, Kanters JA, et al. Water molecules hydrogen binding to aromatic acceptors of amino acids: the structure of Tyr-Tyr-Phe dihydrate and a crystallographic database study on peptides. Acta Cryst D. 1998;54:25–31.
[11] Tóth G, Watts CR, Murphy RF, et al. Significance of aromatic-backbone amide interactions in protein structure. Proteins Struct Funct Genet. 2001;43:373–381.
[12] Hudson KL, Bartlett GJ, Diehl RC, et al. Carbohydrate-aromatic interactions in proteins. J Am Chem Soc. 2015;137:15152–15160.
[13] Makhatadze GI, Privalov PL. Energetics of interactions of aromatic hydrocarbons with water. Biophys Chem. 1994;50:285–291.
[14] Gallicchio E, Zhang LY, Levy RM. The SGB/NP hydration free energy model based on the surface generalized Born solvent reaction field and novel nonpolar hydration free energy estimators. J Comput Chem. 2002;23:517–529.
[15] Takahashi H, Suzuoka D, Morita A. Why is benzene soluble in water? Role of OH/π interaction in solvation. J Chem Theory Comput. 2015;11:1181–1194.
[16] Takahashi H, Matubayasi N, Nakahara M, et al. A quantum chemical approach to the free energy calculations in condensed systems: the QM/MM method combined with the theory of energy representation. J Chem Phys. 2004;121:3989–3999.
[17] Takahashi H, Omi A, Morita A, et al. Simple and exact approach to the electronic polarization effect on the solvation free energy: formulation for quantum-mechanical/ molecular-mechanical system and its applications to aqueous solutions. J Chem Phys. 2012;136:214503.

[18] Warshel A, Levitt M. Theoretical studies of enzymic reactions: dielectric, electrostatic and steric stabilization of the carbonium ion in the reaction of lysozyme. J Mol Biol. 1976;103:227–249.
[19] Warshel A. Computer modeling of chemical reactions in enzymes and solutions. New York (NY): Willey; 1991.
[20] Gao J, Xia X. A priori evalution of aqueous polarization effects through Monte Carlo QM-MM simulations. Science. 1992;258:631–635.
[21] Matubayasi N, Nakahara M. Theory of solutions in the energetic representation. I. Formulation. J Chem Phys. 2000;113:6070–6081.
[22] Suzuoka D, Takahashi H, Morita A. Computation of the free energy due to electron density fluctuation of a solute in solution: a QM/MM method with perturbation approach combined with a theory of solutions. J Chem Phys. 2014;140:134111.
[23] Tomasi J, Mennucci B, Cammi R. Quantum mechanical continuum solvation models. Chem Rev. 2005;105:2999–3093.
[24] Matubayasi N, Nakahara M. Theory of solutions in the energy representation. II. Functional for the chemical potential. J Chem Phys. 2002;117:3605–3616.
[25] Sakuraba S, Matubayasi N. Distribution-function approach to free energy computation. J Chem Phys. 2011;135:114108
[26] Hansen P, McDonald IR. Theory of simple liquids. 3rd ed. London: Academic; 2006.
[27] Frisch MJ, Trucks GW, Schlegel HB, et al. Gaussian 09 revision c01. Wallingford (CT): Gaussian; 2010.
[28] Becke AD. Densityfunctional thermochemistry. III. The role of exact exchange. J Chem Phys. 1993;98:5648–5652.
[29] Dunning TH. Gaussian basis sets for use in correlated molecular calculations. I. The atoms boron through neon and hydrogen. J Chem Phys. 1989;90:1007–1023.
[30] Hohenberg P, Kohn W. Inhomogeneous electron gas. Phys Rev. 1989;136:B864–B871.
[31] Kohn W, Sham LJ. Self-consistent equations including exchange and correlation effects. Phys Rev. 1965;140:A1133–A1138.
[32] Chelikowsky JR, Troullier N, Saad Y. Finite-difference-pseudopotential method: electronic structure calculations without a basis. Phys Rev Lett. 1994;72:1240–1243.
[33] Chelikowsky JR, Troullier N, Wu K, et al. Higher-order finite-difference pseudopotential method: an application to diatomic molecules. Phys Rev B. 1994;50:11355–11364.
[34] Takahashi H, Hori T, Wakabayashi T, et al. A density functional study for hydrogen bond energy by employing real space grids. Chem Lett. 2000;29:222–223.
[35] Takahashi H, Hori T, Wakabayashi T, et al. Real space ab initio molecular dynamics simulations for the reactions of OH radical/OH anion with formaldehyde. J Phys Chem A. 2001;105:4351–4358.
[36] Takahashi H, Hori T, Hashimoto H, et al. A hybrid QM/MM method employing real space grids for QM water in the TIP4P water solvents. J Comput Chem. 2001;22:1252–1261.
[37] Kleinman L, Bylander DM. Efficacious form for model pseudopotentials. Phys Rev Lett. 1982;48:1425–1428.
[38] Ono T, Hirose K. Timesaving double-grid method for real-space electronic-structure calculations. Phys Rev Lett. 1999;82:5016–5019.
[39] Becke AD. Density-functional exchange-energy approximation with correct asymptotic behavior. Phys Rev A. 1988;38:3098–3100.
[40] Lee C, Yang W, Parr RG. Development of the Colle-Salvetti correlation-energy formula into a functional of the electron density. Phys Rev B. 1988;37:785–789.
[41] Allen MP, Tildesley DJ. Computer simulation of liquids. Oxford: Oxford University Press; 1987.
[42] Frankel D, Smit B. Understanding molecular simulation. London: Academc; 1996.
[43] Berendsen HJC, Grigera JR, Straatsma TP. The missing term in effective pair potentials. J Phys Chem. 1987;91:6269–6271.
[44] Scott WRP, Hünenberger PH, Tironi IG, et al. The GROMOS biomolecular simulation program package. J Phys Chem A. 1999;103:3596–3607.
[45] Jorgensen WL, Maxwell DS, Tirado-Rives J. Development and testing of the OPLS all-atom force field on conformational energetics and properties of organic liquids. J Am Chem Soc. 1996;118:11225–11236.
[46] Champagne B, Perpete EA, van Gisbergen SJ, et al. Assessment of conventional density functional schemes for computing the polarizabilities and hyperpolarizabilities of conjugated oligomers: an ab initio investigation of polyacetylene chains. J Chem Phys. 1998;109:10489–10498.
[47] König G, Mei Y, Pickard FC, et al. Computation of hydration free energies using the multiple environment single system quantum mechanical/molecular mechanical method. J Chem Theory Comput. 2016;12:332–344.

Appendix 1. Range of the orbital correlation C_{ij}

As shown in Equation (16), the orbital correlation C_{ij} for orbital pair (i, j) is evaluated by an integration of the absolute of the correlation matrix χ_{ij} defined by Equation (15). In this appendix, we discuss the range of the value of C_{ij}. When the polarisation of ith orbital has no correlation with that of jth orbital, it is easy to see that χ_{ij} in Equation (15) becomes zero. Then, C_{ij} of Equation (16) also takes the minimum value of zero. On the contrary, when we assume that ith orbital perfectly correlates with jth orbital (this situation occurs in the case of $i = j$), the first term of the right-hand side in Equation (15) can be rewritten as

$$\left\langle \hat{\rho}_i\left(\eta_i\right)\hat{\rho}_j\left(\eta_j\right)\right\rangle_0 = \rho_{0,i}\left(\eta_i\right)\delta\left(\eta_i-\eta_j\right). \tag{A1}$$

It is, then, possible to express the correlation matrix χ_{ij} in terms of the distribution function $\rho_{0,i}$, thus,

$$\chi_{ij}\left(\eta_i,\eta_j\right) = \rho_{0,i}\left(\eta_i\right)\delta\left(\eta_i-\eta_j\right) - \rho_{0,i}\left(\eta_i\right)\rho_{0,j}\left(\eta_j\right). \tag{A2}$$

By substituting Equation (A2) into Equation (16) we have the expression for the element C_{ij} at the perfect correlation, which reads

$$\begin{aligned} C_{ij} &= \int \mathrm{d}\eta_i\mathrm{d}\eta_j \left|\chi_{ij}\left(\eta_i,\eta_j\right)\right| \\ &= \int \mathrm{d}\eta_i\mathrm{d}\eta_j \left|\rho_{0,i}\left(\eta_i\right)\delta\left(\eta_i-\eta_j\right) - \rho_{0,i}\left(\eta_i\right)\rho_{0,j}\left(\eta_j\right)\right| \\ &= \int \mathrm{d}\eta_i\mathrm{d}\eta_j\rho_{0,i}\left(\eta_i\right)\left|\delta\left(\eta_i-\eta_j\right) - \rho_{0,j}\left(\eta_j\right)\right| \\ &= \int \mathrm{d}\eta_i\left(\rho_{0,i}\left(\eta_i\right)\left(1-\rho_{0,i}\left(\eta_i\right)\right)\right) \\ &\quad + \int \mathrm{d}\eta_i\mathrm{d}\eta_j\rho_{0,i}\left(\eta_i\right)\rho_{0,j}\left(\eta_j\right) - \int \mathrm{d}\eta_i\rho_{0,i}\left(\eta_i\right)^2 \\ &= 2\left(1-\int \mathrm{d}\eta_i\left(\rho_{0,i}\left(\eta_i\right)\right)^2\right). \end{aligned} \tag{A3}$$

We note that the integration in the parenthesis in the right-hand side of the last equality in Equation (A3) is usually rather small as long as the distribution $\rho_{0,i}$ is broad on the axis of energy η_i. Actually, it can be readily proved that the integration goes to zero at the limit that the distribution is infinitely broadened. In the case of the benzene molecule in our QM/MM simulation, the maximum value of the integration was found to be only 0.016 and, hence, C_{ij} takes values very close to 2.0 on the diagonal of the correlation matrix.